SAGE-Hindawi Access to Research
International Journal of Alzheimer's Disease
Volume 2011, Article ID 962352, 13 pages
doi:10.4061/2011/962352

Research Article

Cell Surface Binding and Internalization of Aβ Modulated by Degree of Aggregation

David A. Bateman[1] and Avijit Chakrabartty[2, 3, 4]

[1] *Laboratory of Biochemistry and Genetics, National Institute of Diabetes, Digestive and Kidney Diseases, National Institutes of Health, Bethesda, MD 20892-0830, USA*
[2] *Department of Medical Biophysics, University of Toronto, Toronto, ON, Canada M5G 1L7*
[3] *Department of Biochemistry, University of Toronto, Toronto, ON, Canada M5G 1L7*
[4] *MaRS Centre, Toronto Medical Discovery Tower, 4th Floor Rm 4-307, 101 College Street, Toronto, ON, Canada M5G 1L7*

Correspondence should be addressed to Avijit Chakrabartty, chakrab@uhnres.utoronto.ca

Received 12 August 2010; Revised 4 November 2010; Accepted 14 December 2010

Academic Editor: Anne Eckert

The amyloid peptides, Aβ40 and Aβ42, are generated through endoproteolytic cleavage of the amyloid precursor protein. Here we have developed a model to investigate the interaction of living cells with various forms of aggregated Aβ40/42. After incubation at endosomal pH 6, we observed a variety of Aβ conformations after 3 (Aβ^{3}), 24 (Aβ^{24}), and 90 hours (Aβ^{90}). Both A$\beta 42^{24}$ and A$\beta 40^{24}$ were observed to rapidly bind and internalize into differentiated PC12 cells, leading to accumulation in the lysosome. In contrast, A$\beta 40/42^{90}$ were both found to only weakly associate with cells, but were observed as the most aggregated using dynamic light scattering and thioflavin-T. Internalization of A$\beta 40/42^{24}$ was inhibited with treatment of monodansylcadaverine, an endocytosis inhibitor. These studies indicate that the ability of Aβ40/42 to bind and internalize into living cells increases with degree of aggregation until it reaches a maximum beyond which its ability to interact with cells diminishes drastically.

1. Introduction

Alzheimer's disease (AD) is a progressive neurological disorder resulting from the deposition of Alzheimer β-Amyloid peptide (Aβ) as senile plaques, the appearance of neurofibrillary tangles, and selective neuronal loss. The most abundant forms of Aβ are 40 and 42 amino acid residues long and referred to as Aβ40 and Aβ42, respectively [1].

The endocytic pathway has been implicated in the extracellular secretion of Aβ40 and Aβ42 [2, 3]. These peptides are derived from the endoproteolytic cleavage of the Amyloid precursor protein (APP) with β-secretase, followed by γ-secretase. β-secretase cleavage occurs in the acidic late endosomes [4, 5]. After γ-secretase cleavage, Aβ40 or Aβ42 is free in the endosomal lumen [6]. The endosomal contents can be either secreted from the cell [7–9] or transferred to the lysosome [10].

The endosome has been found to be quite acidic (pH 6) with the recycled endosome slightly less acidic (pH 6.5) [11, 12]. Exposure of Aβ to endosomal pH conditions has been found to induce various conformational and oligomeric states [13–15]. Many oligomeric forms of Aβ have been proposed and characterized as intermediates in the pathway to forming the Amyloid fibre. Some of these structures include trimers, pentamers, high molecular weight Aβ-derived diffusible ligands (ADDLs), protofibrils, and fibrils [16–21].

Here we present a method for generating a mixed population of Aβ conformations using model endocytic conditions. Using this method, we demonstrate that when Aβ is exposed to endosomal conditions for an extended period of time, the ability of the peptide to bind and internalize into living rat adrenal pheochromocytoma (PC12) cells increases with time until it reaches a maximum beyond which its ability to interact with PC12 cells diminishes drastically.

2. Materials and Methods

2.1. Peptide Synthesis and Purification. Aβ40 and Aβ42 were synthesized and purified as described previously [22]. Before cleavage from the resin, the fluorophore, Nα-(9-Fluorenylmethoxycarbonyl)-Nε-tetramethylrhodamine-(5-carbonyl)-L-lysine (Molecular Probes, Eugene, OR) (abbreviated TMR), was coupled to the N-terminus via a glycine linker. The crude peptides were purified by HPLC using a Superdex Tricorn 10/300 GL Peptide column (Amersham Biosciences, Piscataway, NJ) with 30 mM NH_4OH running buffer. To maintain stock peptide solutions free from fibril seeds, solutions were stored at pH 10 and 4°C immediately after chromatographic separation of monomeric peptides. Aβ preparations were never lyophilized, as this process may allow for seeds to form. These solution conditions have been previously shown to maintain the monomeric state [16, 23, 24]. Peptide purity and identity was confirmed using both MALDI mass spectrometry and amino acid analysis. Concentrations of stock peptide solutions were determined using amino acid analysis and confirmed by either tyrosine absorbance (275 nm, $\varepsilon = 1390\,\text{cm}^{-1}\,\text{M}^{-1}$) or TMR absorbance for labelled peptides (550 nm, $\varepsilon = 92000\,\text{cm}^{-1}\,\text{M}^{-1}$). At least three separate synthesized lots of Aβ were used in this study and each displayed identical cell association rates when compared for quality assurance. Oligomeric samples were prepared by diluting stock Aβ samples to 30 μM with 30 mM NH_4OH and reducing to pH 6 with 0.2 M HCl and incubating for zero (Aβ^0), 3 (Aβ^3), 24 (Aβ^{24}), or 90 hours (Aβ^{90}) in the dark at 20°C.

2.2. Dynamic Light Scattering (DLS). Hydrodynamic radius (Rh) measurements were made at 20°C with a DynaPro DLS instrument (Protein Solutions Inc., Piscataway, NJ). Peptide samples (30 μM) were reduced to pH 6 using 0.2 mM HCl, centrifuged at 12000 ×g for 3 minutes and then rapidly added to a 1 cm path length cuvette and left in the instrument. DLS data was collected at various time points over 90 hours. Particle translational diffusion coefficients were calculated from decay curves of autocorrelation of light scattering data and converted to hydrodynamic radius (Rh) with the Stokes-Einstein equation. Histograms of intensity versus Rh were calculated using Dynamics data analysis software (Protein Solutions Inc., Piscataway, NJ).

2.3. Filter Assay. Aβ samples (30 μM) were either not filtered or spin-filtered for 30 minutes at 14,000 ×g using 10, 30, 100 kDa (Amicon ultra cellulose KMWO), or 0.1 μm (Amicon PVDF) spin filters. Absorbance at 550 nm was collected on a Molecular Devices SpectraMax M5 (Molecular Devices Corp., Sunnyvale, CA) and graphs were created normalizing the absorbance signal from each filtered sample to the corresponding unfiltered sample.

2.4. Thioflavin-T Assay. Fluorescence measurements were obtained using 200 μL of 30 μM Aβ samples, within a 96-well plate, after addition of 5-fold molar excess of thioflavin-T and incubation at room temperature for 30 minutes. Emission at 485 nm was collected using 440 nm excitation on a Molecular Devices SpectraMax M5 (Molecular Devices Corp., Sunnyvale, CA).

2.5. Cell Culture. PC12 cells were maintained in DMEM/F12 containing 10% fetal bovine serum (HyClone, Logan, UT) with 100 units/mL penicillin and 100 μg/mL of streptomycin. To induce differentiation of PC12 cells and for cell imaging, they were plated at 2.2×10^4 cells/cm^2 in Lab-tech chambered cover glass chambers and suspended in phenol red free DMEM/F12 containing N2 supplement and 10 ng/mL NGF. Cells were differentiated for 72 hours before media was replaced and peptide treatments (final concentration 1.5 μM) were performed. Cells were maintained at 37°C in a humidified incubator with 5% carbon dioxide.

2.6. Analytical Ultracentrifugation. TMR-labelled Aβ samples (6 μM) were prepared in phenol red free DMEM/F12 media containing N2 supplement and 10 ng/mL NGF. Either fresh media or cultured supernatants, obtained from cell culture after 72 hours, were used. To avoid interference from cell culture components, molecular weights of TMR-labelled Aβ were obtained by selective monitoring of TMR absorbance at 550 nm. Sedimentation experiments were performed at 20°C on a Beckman XLI analytical ultracentrifuge using an AN50-Ti rotor. Molecular weights were calculated using Beckman XLI data analysis software in which absorbance versus radial position data were fitted to the sedimentation equilibrium equation using nonlinear least-squares fitting.

2.7. Confocal Microscopy. Three-dimensional stacks of fluorescence micrographs were taken at 20°C with a confocal laser-scanning system consisting of an LSM 510 Zeiss META NLO confocal microscope with a C-APO 40X water immersion objective (numerical aperture 1.2) and HeNe laser with a 543 nm laser line. The displayed images were captured using Zeiss LSM Image version 4 and prepared using ImageJ version 1.37v and represent a single cross-section through the cells.

2.8. Inhibition of Endocytosis. Differentiated PC12 cells were treated with 50 μM monodansylcadaverine (MDC) for 20 minutes at 37°C with 5% carbon dioxide. After inhibitor treatment, Aβ^{24} (final concentration 1.5 μM) was added to the media containing MDC and imaged after 4 hours at 37°C. Aβ^{24} (final concentration 1.5 μM) was also added to differentiated PC12 cells media for 4 hours at either 37°C or 4°C prior to imaging.

2.9. Intracellular Localization. Differentiated PC12 cells were first treated with Aβ^{24} (final concentration 1.5 μM) for 6 hours at 37°C followed by treatment with 40 nM Mito-Tracker Deep Red and 50 nM LysoTracker Green DND-26 for 20 minutes. After treatment, the media was exchanged with fresh phenol red free DMEM/F12 media containing N2 supplement and 10 ng/mL NGF with 1.5 μM DAPI for nuclear staining. Cells were imaged using Argon laser with 488 nm laser line for LysoTracker, HeNe laser with 633 nm

laser line for MitoTracker, HeNe Laser with 543 nm laser for TMR-labelled Aβ^{24}, and a tunable Chameleon laser at 730 nm for two-photon excitation of DAPI. 2D histograms and correlation coefficients were determined using Image J version 1.42q with colocalisation threshold plugin [25].

2.10. Toxicity. Differentiated PC12 cell media was replaced with media containing 0.6 to 20 μM Aβ^{0}, Aβ^{24}, Aβ^{90}, or 10 μM Melitin as a positive control for 48 hours. Cell survival was quantified using the Sulforhodamine B assay [26], and absorbance was measured at 560 nm using Molecular Devices SpectraMax M5 (Molecular Devices Corp., Sunnyvale, CA). LC50 values were determined as the concentration of Aβ required to kill fifty percent of the cells from an absorbance versus Aβ concentration plot.

3. Results

3.1. Aβ Aggregation Is Mediated through Cell Interaction. To study the interaction between Aβ and live cells, we synthesized and fluorescently labelled Aβ40/42. The synthesized Aβ was maintained in solution from purification to storage and was never lyophilized, as these solution conditions are known to significantly reduce the formation of Aβ aggregation seeds [16, 23, 24]. We covalently attached tetramethylrhodamine (TMR) to the N-terminus of Aβ via a flexible glycine linker to generate TMR-Aβ. The N-terminus of Aβ is highly accessible even in the fibril state [21, 27, 28] and attaching a fluorescent label to this site has been shown to neither alter its amyloidogenic properties [16, 29, 30], nor its solubility behaviour [31, 32].

We have previously shown that treating cultured cells with 1.5 μM monomeric TMR-Aβ42 leads to the formation of visible aggregates on the surface of PC12 cells within one hour of treatment [29]. We initiated our current study by investigating whether Aβ aggregation could occur in cell culture media alone. Using analytical ultracentrifugation, we measured the molecular weights of Aβ40 and Aβ42 present in phenol red free cell culture medium, both freshly prepared and conditioned media taken from differentiated PC12 cells 3 days postdifferentiation. Following the addition of 6 μM Aβ to each medium and subsequent 24-hour incubation at room temperature, both media preparations were centrifuged to equilibrium at room temperature in an analytical ultracentrifuge in order to determine the molecular weight of Aβ conformations. The molecular weights of Aβ40 and Aβ42 from both media preparations were measured to be approximately 4103 Da and 4425 Da, respectively. These values both correspond to the expected monomeric molecular weights of Aβ, falling within the 95% confidence intervals of 3650–4570 Da for Aβ40 and 3650–4770 Da for Aβ42. Thus, the aggregation of Aβ seen by confocal microscopy apparently occurs only after interaction with the differentiated PC12 cells and not with cultured supernatants. It should be noted that the concentration previously used to treat cells (1.5 μM) and the concentration used for ultracentrifugation (6 μM) are considerably lower than the reported 20 to 50 μM range required for *in vitro* aggregation [33–35].

3.2. Aβ Oligomerizes at Endosomal pH. We have previously shown that Aβ40 and Aβ42 aggregate significantly at pH 6 [29]. Since Aβ40 and Aβ42 are generated through endoproteolytic cleavage [7–9], and the pH of the endosome and recycled cellular vesicles is equivalent to pH 6 [12], we characterized the Aβ conformations formed under endosome conditions. Aβ (30 μM) was reduced to pH 6, and hydrodynamic radius calculations were collected after zero (Aβ^{0}), 3 (Aβ^{3}), 24 (Aβ^{24}), and 90 (Aβ^{90}) hours using dynamic light scattering (Figure 1). The average hydrodynamic radius of Aβ40 was found to increase from 2.0 nm at time zero (Aβ40^{0}) to 216 nm after 90 hours at pH 6 (Aβ40^{90}). A more striking increase was found with Aβ42, beginning with 1.7 nm at time zero (Aβ42^{0}) to 451 nm after 90 hours at pH 6 (Aβ42^{90}). For each of these samples, the development of increasingly higher ordered aggregates was observed over time and the samples that were treated for 90 hours contained particles over 1000 nm in radii.

To further investigate the relative levels of peptide aggregation at endocytic pH, we filtered the Aβ40 and Aβ42 samples through various molecular weight cutoff (MWCO) spin filters (Figure 2). Approximately 67% of Aβ40^{3}, 60% of Aβ40^{24}, and 55% of Aβ40^{90} were recovered through the 10 kDa MWCO spin filter and approximately 80% were recovered through the 100 kDa MWCO filter, except for Aβ40^{90} with only 60% recovered. In contrast, only 55% of Aβ42^{3}, Aβ42^{24}, and Aβ42^{90} were recovered through the 10 kDa filter and approximately 60% were recovered through the 100 nm filter. These results indicate that the majority of peptide conformations present under these conditions were able to pass through a 10 kDa molecular weight filter, but that just over 40% could not be recovered through the 100 nm filter for the Aβ40^{90}, Aβ42^{3}, Aβ42^{24}, and Aβ42^{90} samples.

We also used thioflavin-T to assess the time-dependence of the extent of Amyloid fibril formation at endocytic pH. Thioflavin-T is a dye known to shift its fluorescence from 430 nm to 490 nm upon binding specifically to the cross-β-structure of Amyloids but not to monomeric or small oligomeric complexes [36, 37]. We observed enhanced thioflavin-T fluorescence at all time points (Figure 3); however, Thioflavin-T bound most strongly to Aβ40^{90}, Aβ42^{24}, and Aβ42^{90}. The high thioflavin-T binding to Aβ^{90} samples suggests that these late stage Aβ conformations are the most aggregated.

3.3. Endocytic Aβ Undergoes Rapid Cellular Interaction. Using confocal microscopy, cell surface association and internalization of peptides can be monitored. We have previously shown that monomeric Aβ42 associates with cells more rapidly than Aβ40, with significant staining observable after six hours of treatment [29]. To determine whether the aggregation state of Aβ affects cell association, we exposed each of the Aβ40 and Aβ42 samples to differentiated PC12 cells and monitored the kinetics of association by confocal microscopy. Upon treating cells with Aβ40^{24}, the cell surface association was observed within one hour of treatment (Figure 4). Moreover, Aβ40^{24} was observed to significantly internalize into these cells after only 6 hours, whereas significant internalization of Aβ40^{0} was only visualized around

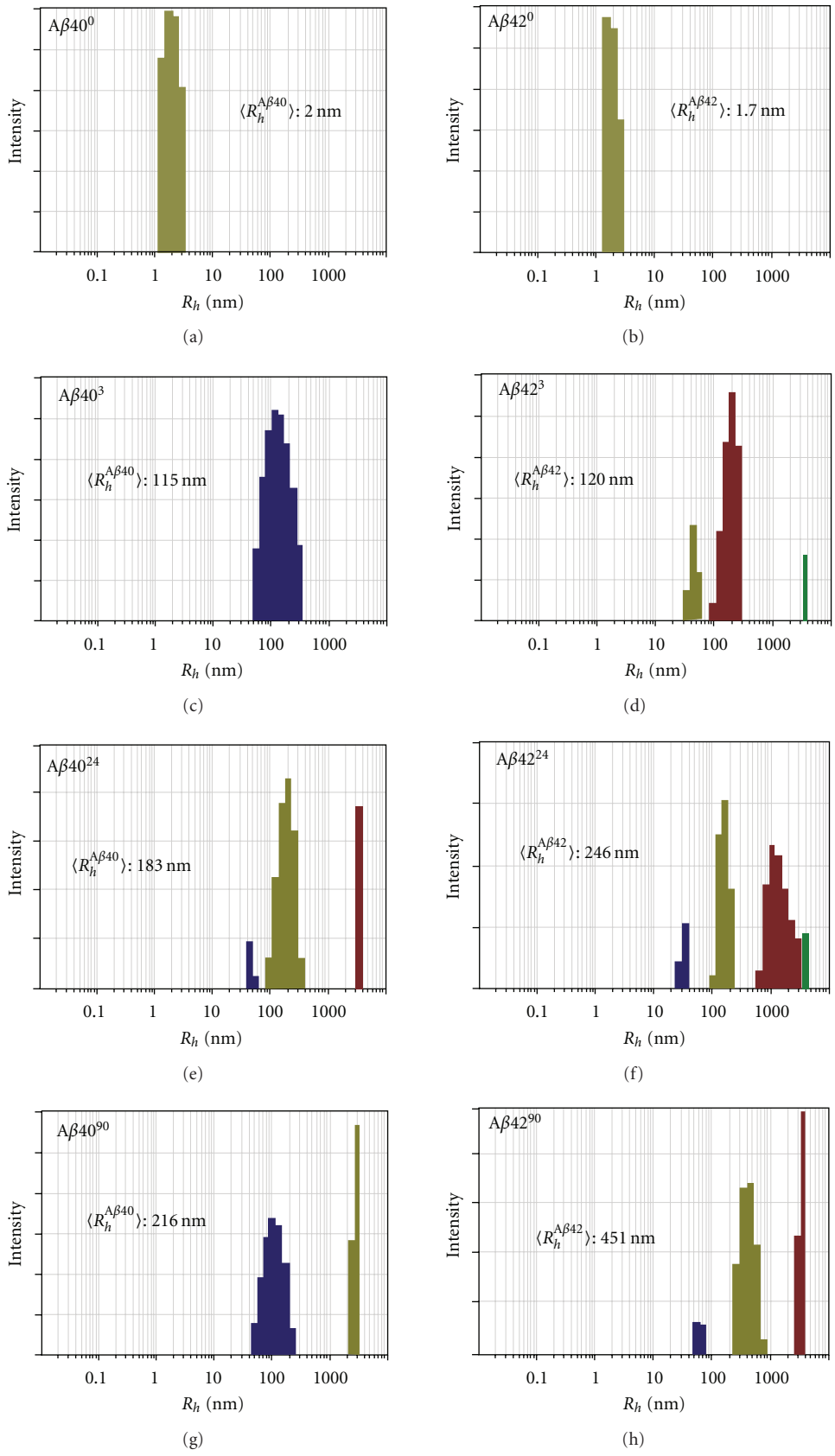

Figure 1: Dynamic light scattering of endocytic Aβ. A time-dependent increase in the average hydrodynamic radius (R_h) was observed with incubation of Aβ under endocytic conditions. At each time point, a variety of aggregates are present.

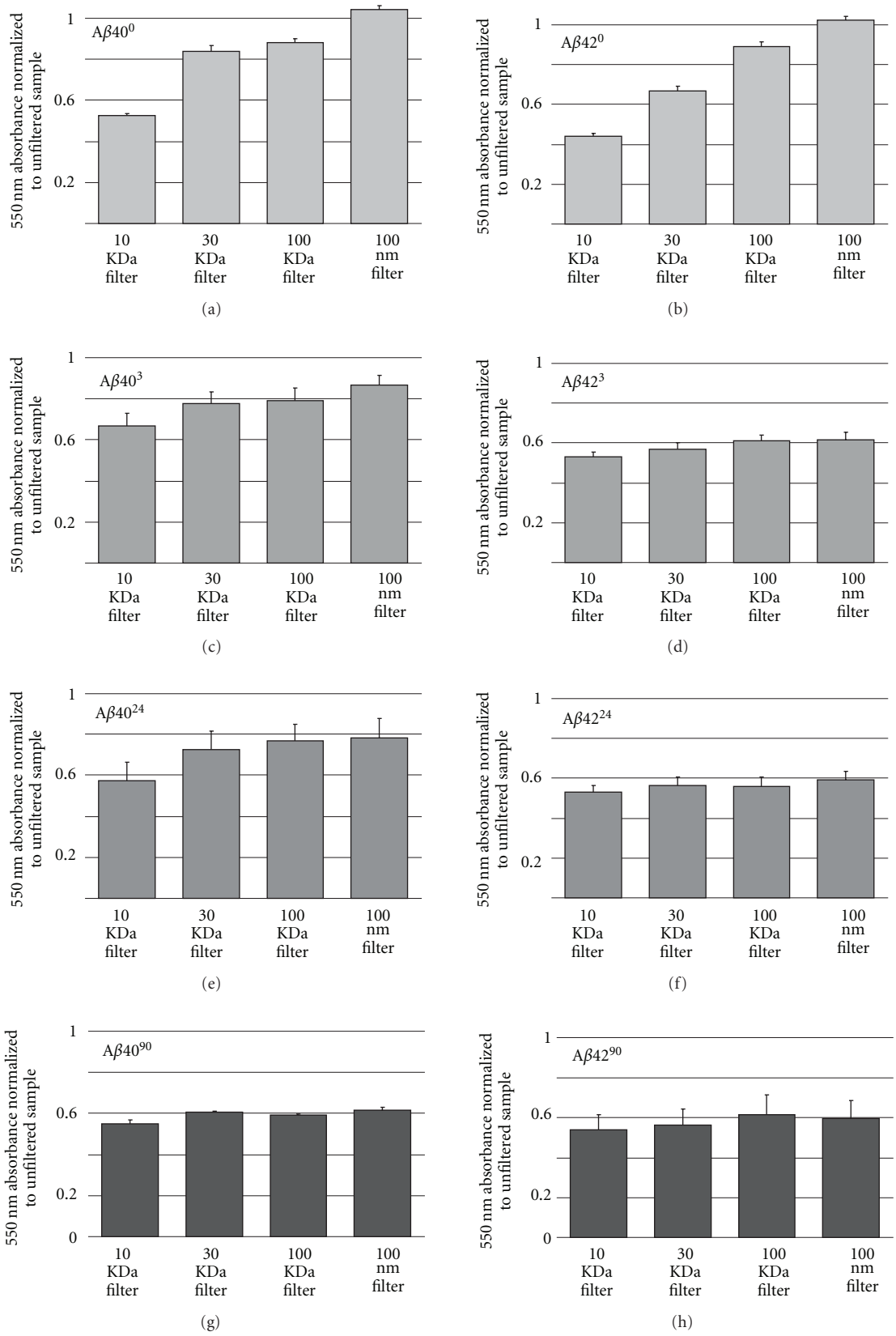

Figure 2: Separation of Aβ by ultrafiltration. Graphs show the TMR absorbance of the filtrates for each Aβ sample divided by the absorbance of the unfiltered sample at 550 nm. Error bars represent the range from two independent experiments.

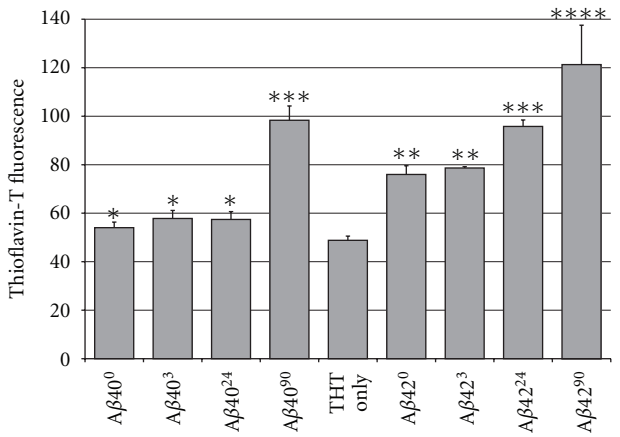

FIGURE 3: Thioflavin-T fluorescence of Aβ exposed to endocytic conditions. Significant thioflavin-T fluorescence for the Aβ40^{90} and Aβ42^{90} samples indicates the highest level of aggregation present. Error bars represent the range of two independent experiments. Statistical significance is indicated (*) $P < .05$.

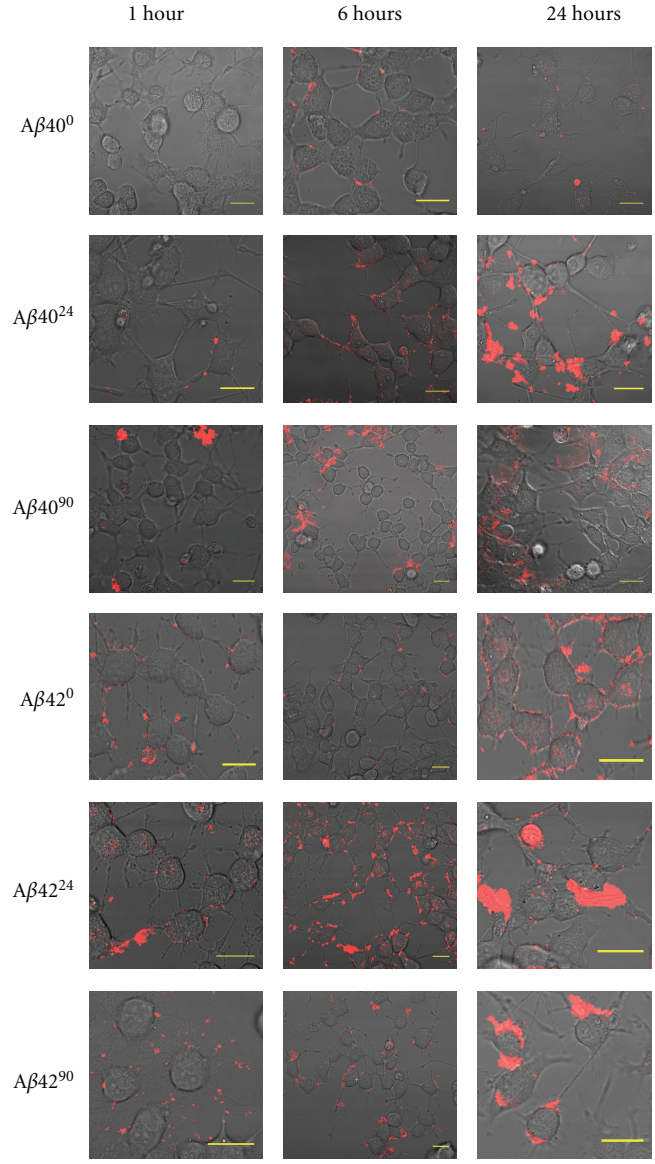

FIGURE 4: Confocal Microscopy images showing Aβ time course of cell entry. Confocal microscopy images of differentiated PC12 cells treated with various Aβ samples exposed to endosomal conditions after 1, 6, and 24 hours. All scale bars are 20 μm in length. Aβ40^{24} associates rapidly to differentiated PC12 compared to Aβ40^{0}, whereas Aβ40^{90} displays weak cell association over its treatment course. Aβ42^{24} displays rapid internalization compared to Aβ42^{0}. Aβ42^{90} displays reduced cell interaction compared to Aβ42^{0} and Aβ42^{24}.

24 hours (Figure 4). Similarly, Aβ42^{24} internalized into differentiated PC12 cells after only one hour of treatment, whereas Aβ42^{0} treatment only became observable at 24 hours (Figure 4). Interestingly, when differentiated PC12 cells were treated with late-stage Aβ40^{90} or Aβ42^{90}, very few cells underwent internalization or even exhibited cell surface interaction with these aggregated peptide forms (Figure 4). To illustrate the contrast between these treatments, we collected the three-dimensional image slices through a cell from the base to the apex for the 6-hour treatment with Aβ42^{0}, Aβ42^{24}, and Aβ42^{90} (Figure 5). Aβ42^{0} was only observed around the periphery of the cell, whereas some Aβ42^{24} was located inside the cell. By contrast, Aβ42^{90} treatment seemed to localize to extracellular regions and did not produce the punctate pattern as observed with the Aβ42^{0} sample.

To quantify the frequency of cells that exhibited peptide internalization, we randomly selected five fields of view from at least three separate 6-hour treatment experiments and plotted the percentage of cells having internalized Aβ (Figure 6). Approximately 25% of cells internalized Aβ40/42^{3}, whereas more than 90% of cells internalized Aβ40/42^{24}. In contrast, very few cells were found to internalize Aβ40/42^{90}. Since late Aβ40/42^{90} was found to have a large number of aggregates with hydrodynamic radius over 1000 nm (Figure 1) and were found to significantly bind thioflavin-T (Figure 3), then these aggregates may favour self-association over cell association.

3.4. Internalization of Aβ Is Mediated through Cellular Import Mechanisms. To determine if the internalization of endocytic Aβ is mediated through cellular processes, such as receptor-mediated endocytosis or through direct peptide-mediated processes like membrane pore formation, we monitored the effects of temperature and monodansylcadaverine (MDC) on internalization. MDC is a known inhibitor of receptor-mediated clathrin-dependent endocytosis [38, 39]. At physiological temperature (37°C), after a 4-hour treatment of cells with Aβ40^{24} and Aβ42^{24}, internalization was observed (Figure 7). At 4°C membrane vesicle formation is inhibited, preventing endocytosis of extracellular and cell surface components [40]. When Aβ40^{24} or Aβ42^{24} association with differentiated PC12 cells was monitored at 4°C, none of the cells were found to have internalized these peptides

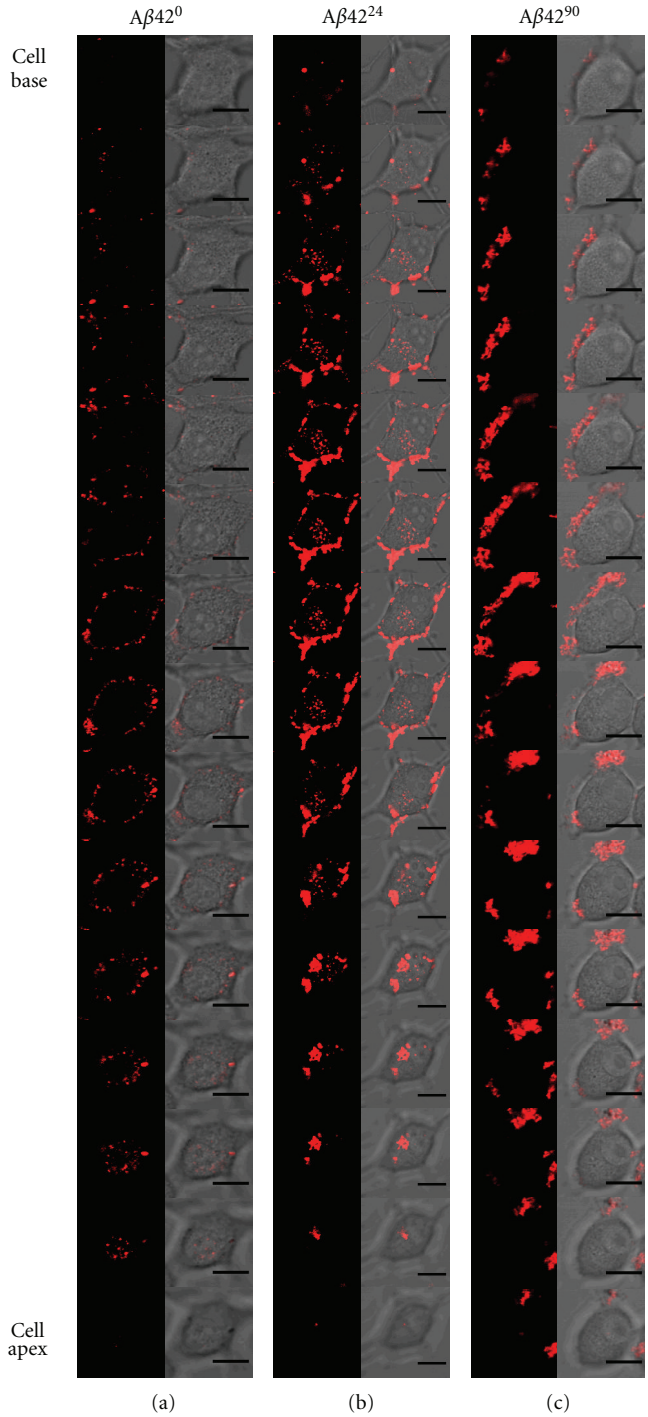

FIGURE 5: Image planes though a single cell for each Aβ42 treatment. Confocal microscopy images from differentiated PC12 cell base to cell apex for Aβ42^0, Aβ42^{24}, and Aβ42^{90}, with the TMR signal only (a) and TMR cell merged image (c). All scale bars are 10 μm in length.

(Figure 7). Similarly, when differentiated PC12 cells were treated with MDC, neither Aβ40^{24} nor Aβ42^{24} were observed within the cells. These observations indicated that Aβ^{24} was internalized through a cell-directed import mechanism, rather than an independent penetration route through the cell membrane.

3.5. Internalized Aβ Is Targeted to the Lysosome. The location of deposited intracellular Aβ40/42^{24} was examined using intracellular organelle markers in differentiated PC12 cells. Cells treated with Aβ40^{24} and Aβ42^{24} for 6 hours were visualized using LysoTraker Green DND-26 for the lysosome, MitoTracker Deep Red for the mitochondria, and DAPI for

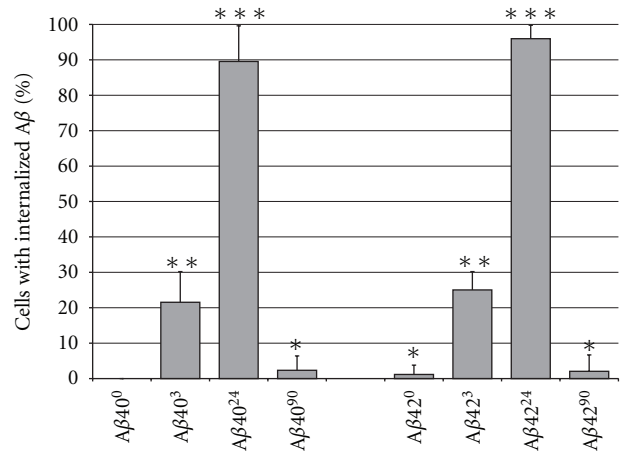

FIGURE 6: Percentage of PC12 cells with internalized Aβ. Aβ40^{24} and Aβ42^{24} were more significantly internalized into differentiated PC12 cells than the other forms of Aβ. Aβ40^{90} and Aβ42^{90} display a striking drop in the amount of internalization. Error bars represent the standard deviation from at least three individual experiments with $n > 200$ cells per condition. Statistical significance is indicated (*) $P < .005$.

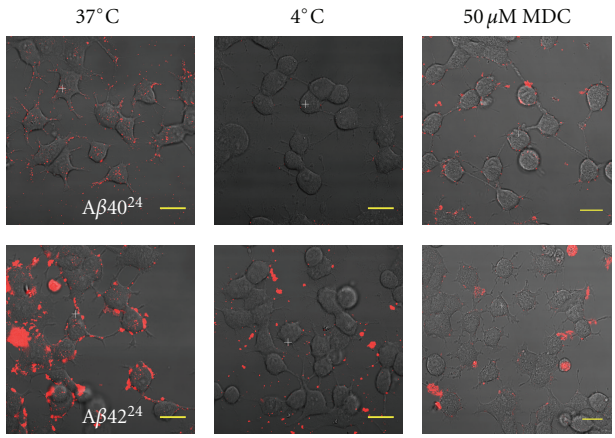

FIGURE 7: Inhibition of Aβ internalization. Confocal microscopy images of differentiated PC12 cells treated with Aβ40/42^{24} for 4 hours. All scale bars are 20 μm in length. Internalization was only observed at 37°C. Membrane integrity was maintained throughout all treatments, indicating that internalization is mediated through a cellular process such as clathrin-dependent endocytosis.

nucleus staining (Figure 8). The staining pattern of each cellular organelle marker in the same image plane as the Aβ40^{24} and Aβ42^{24} treatment was determined (Figure 8) and quantified (Figure 9). Only the signal from the lysosome marker costained with both internalized Aβ40^{24} and Aβ42^{24}. The red signal from the peptides costained well with green signal from the lysosomes, resulting in the yellow signal in the merged image. When quantified, 71% of the lysosome signal intensity colocalised with the Aβ40 channel and 80% with the Aβ42 channel (Figure 9). Whereas only 9% of the mitrochondria signal intensity colocalised with Aβ40 channel and less than 1% with the Aβ42 channel (Figure 9). These findings suggest that the internalized vesicles containing Aβ40/42^{24} are directed to the lysosome. The intensity of both Aβ40^{24} and Aβ42^{24} fluorescence signals was found to increase in the lysosomes over time, which may reflect the accumulation of Aβ40/42^{24} in the lysosome.

To determine the relative toxicity of these Aβ conformations, a cytotoxicity assay was performed where differentiated PC12 cells were treated with various peptide concentrations for 48 hours (Figure 10). We calculated the lethal concentration at which 50% of cells were killed (LC50), for each of the Aβ conformations. We found that Aβ40^{24} was moderately more toxic than Aβ40^{0}, with a lower LC50 value (Figure 10). Surprisingly, Aβ40^{90} was also found to have a lower LC50 value compared to Aβ40^{0}. Aβ42^{24} was also found to be moderately more toxic than Aβ42^{0}, whereas Aβ42^{90} had a much higher LC50 value compared to Aβ42^{0} (Figure 10).

4. Discussion

We have developed a method to produce a collection of Aβ conformations that differ in their extent of aggregation and investigated the interaction between these states of Aβ40 and Aβ42 and differentiated PC12 cells. Others have described the methods to isolate individual soluble oligomeric forms of Aβ, using various chemical reagents and protocols [41–44]. In addition, purified oligomeric Aβ molecules from cell culture [45, 46] or transgenic mice [47] have also been monitored. These purified sources of oligomeric Aβ offer great potential in understanding the progression of Aβ aggregation; however, they cannot be directly visualized over the time course of their effects on cells during maturation from earlier to later conformations. Since it is well established that Aβ monomers can oligomerize under the physiological pH of the endosome [13–15], and Aβ is formed through endoproteolytic cleavage, we have utilized this condition to determine which conformations are present and how these mixed conformations interact with differentiated PC12 cells. It is known that the extent of oligomerization/fibrillation is very dependent on experimental conditions. Necula et al. [48] have indicated that Aβ can be induced to form fibrils via dilution from 100 mM NaOH to neutral pH in the presence of 10 mM HEPES/100 mM NaCl buffer, while dilution into phosphate buffered saline results in oligomer formation. In our experiments, the peptide was diluted from 30 mM ammonium hydroxide (pH 10) to pH 6 with final condition of 1 mM ammonium chloride as the only additional chemical. We do note that the normal human physiological concentration of ammonium chloride in blood and cerebrospinal fluid is approximately 20 to 50 μM [49, 50], and that hyperammonemia has been linking to Alzheimer type II astrocytosis [51, 52].

When extracellular monomeric Aβ associates to the surface of cells, we speculate there are three possible outcomes: (1) it can act as a stable template to allow further Aβ aggregation; (2) the peptide can penetrate through the cell membrane depositing in the cytoplasm; or (3) the peptide may be internalized into the cell within endocytic vesicles, which would result in a reduction in the surrounding pH. In the third case, the endocytic vesicles containing Aβ can

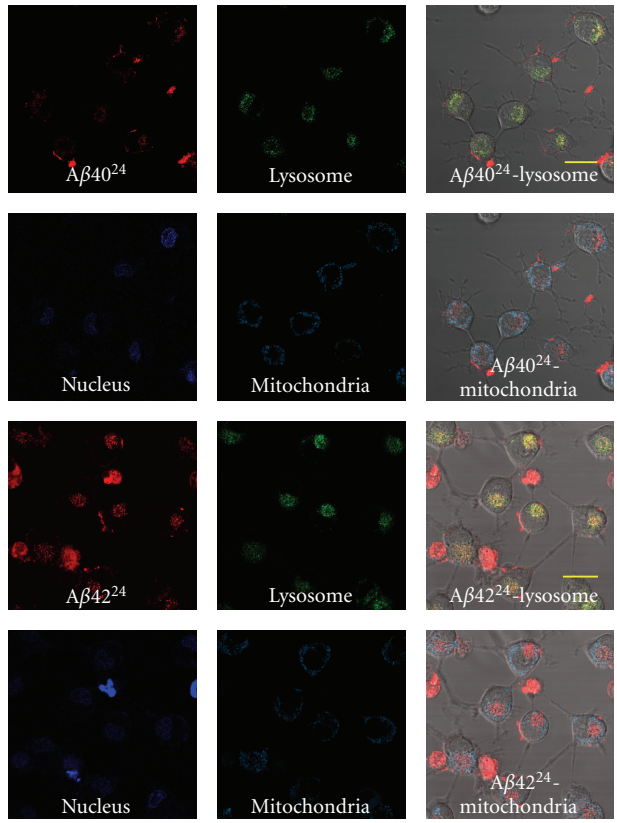

FIGURE 8: Intracellular localization of endocytic Aβ. Confocal microscopy images through a single plane of cells treated with either $A\beta40^{24}$ or $A\beta42^{24}$ and intracellular markers. All scale bars are 20 μm in length. Colocalization between the red $A\beta40/42^{24}$ signal and the green lysosome signal is shown in yellow in the merged image. Colocalization was not observed with either mitochondrial or nuclear stains.

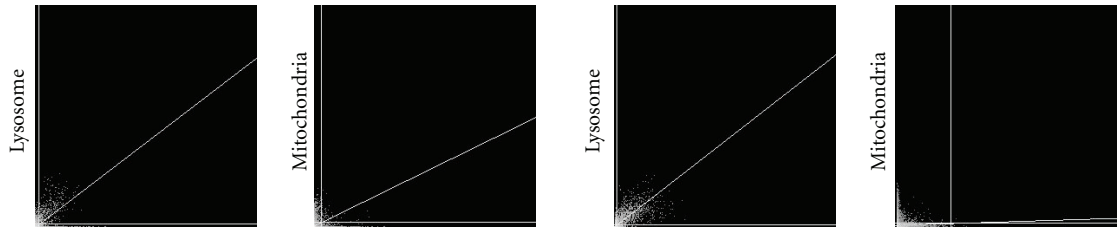

Ch1	Ch2	Pearson's correlation coefficient whole image	m	b	Ch1 threshold	Ch2 threshold	Pearson's correlation coefficient above threshold	Pearson's correlation coefficient below threshold	Mander's coefficient Ch1	Mander's coefficient Ch2	Mander's coefficient Ch1 threshold	Mander's coefficient Ch2 threshold	Ch1 colocalized %	Ch2 colocalized %	Ch1 intensity colocalized %	Ch2 intensity colocalized %
Aβ40	Lysosome	0.356	0.764	−0.3	4	3	0.5323	0.007	0.5355	0.8996	0.4869	0.7578	43.72%	51.55%	43.77%	71.34%
Aβ40	Mitochondria	−0.205	0.49	1.1	8	5	−0.1885	0.009	0.2702	0.6454	0.1539	0.1302	11.33%	9.7%	7.82%	9.24%
Aβ42	Lysosome	0.782	0.781	−1.1	4	2	0.4755	0.054	0.6235	1	0.5736	0.8464	63.02%	57.01%	51.34%	80.61%
Aβ42	Mitochondria	0.01	0.032	1.9	64	4	NA	0.009	0.4781	1	0.1681	0.0008	9.09%	0.07%	0.17%	0.04%

FIGURE 9: Quantitative colocalisation analysis of intracellular Aβ. Quantitative analysis indicates significant colocalisation of $A\beta40^{24}$ and $A\beta42^{24}$ with the lysosome marker within live cells.

theoretically be recycled back to the cell surface or directed to the lysosome where a further reduction in pH would occur. We have previously visualized oligomeric Aβ on the surface of neuronal cell lines [29], and here sought to determine first whether this aggregation occurred prior to cell surface deposition in the cell culture mediaor are aggregation and cell surface binding concomitant and linked processes. Using ultracentrifugation analysis of Aβ preparations either in freshly prepared cell culture media or in conditioned media removed from cultured cells after 3 days, we did not observe any conformation larger than the monomer. These results indicate that components in our cell media or secreted factors from cultured cells are not responsible for the observed Aβ aggregation present on the surface of neuronal cells. After adding monomeric Aβ to cells, we noted a maturation time for the visual appearance of Aβ on

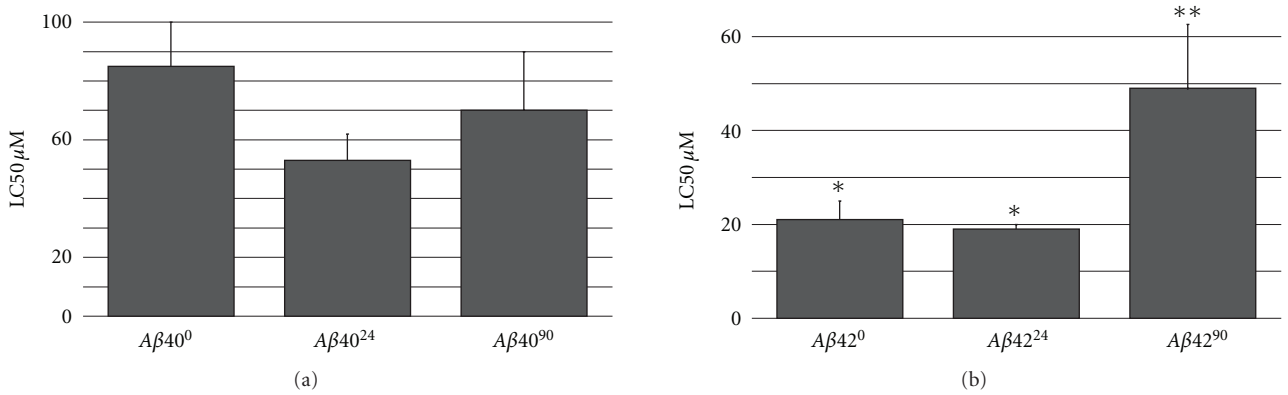

Figure 10: Relative toxicity of endocytic Aβ. Lethal concentration of endocytic Aβ required to kill 50% of differentiated PC12 cells at 48 hours is shown. Error bars represent the standard deviation from the mean using three replicates. Statistical significance is indicated (*) $P < .05$.

the cell surface and in the cell interior (Figure 4; [29]). We postulate that the peptides on the cell surface might undergo a series of pH reductions through endocytic recycling, before becoming visible punctae on and inside the cell. Since pH 6 is approximately endocytic pH, we characterized the kinetic effects of this condition on peptide conformations. Exposing Aβ40 for up to 24 hours at pH 6, we observed an increase in the average hydrodynamic radius from 2.0 nm (A$\beta40^0$) to 183 nm (A$\beta40^{24}$) (Figure 1). In addition, approximately 60% of these peptides were recovered through a 10 kDa MWCO filter and 80% were recovered through a 100 kDa MWCO filter (Figure 2), and only minor thioflavin-T binding was found (Figure 3). Following exposure of up to 24 hours at pH 6, Aβ42 had an increase in the average hydrodynamic radius from 1.7 nm (A$\beta42^0$) to 246 nm (A$\beta42^{24}$) (Figure 1), approximately 55% were recovered through 10 kDa MWCO filter and only 60% were recovered through 100 nm filter (Figure 2) and more significant thioflavin-T binding was measured (Figure 3). Both Aβ40 and Aβ42 treated for 90 hours at pH 6 were observed to have large average hydrodynamic radius particles, with 40% of these samples being withheld by a 100 nm filter and both displayed significant thioflavin-T staining. Also, these early-and late-stage Aβ samples were observed to have an ensemble of Aβ conformations (Figure 1).

The interactions of these early-and late-stage Aβ conformations were monitored with differentiated PC12 cells. Whereas late stage A$\beta40^{90}$ and A$\beta42^{90}$ exhibited very few interactions with cells (Figures 4, 5) and internalized at a very low frequency (Figure 6), early stage A$\beta40^{24}$ and A$\beta42^{24}$ interacted with cells rapidly (Figure 4) and internalized into the majority of the cells present (Figure 6). Interestingly, A$\beta40^{24}$ showed a more rapid cellular association and internalization compared to A$\beta40^0$ (Figure 4). Similarly, A$\beta42^{24}$ was found to internalize more rapidly than A$\beta42^0$, indicating that a specific conformation may play a role in cell binding and internalization. Furthermore, our model of endocytic Aβ toxicity (Figure 10) is in agreement with previous findings utilizing chemically-produced oligomers of Aβ which showed that Aβ fibrils were less toxic than soluble oligomers [41, 53]. Our results with Aβ^{90} are also in agreement with studies that have indicated that regions with large Amyloid plaques do not correlate directly with regions of significant neuronal loss [54, 55].

Many studies have reported that certain oligopeptides are freely imported into cells. For example, the peptide sequences corresponding to Tat (48–60), penetratin, and oligoarginine are known to internalize into live cells. Cellular import of Tat (48–60) and penetratin was shown to be temperature dependent, indicating the possible role of endocytosis for internalization [56, 57]. In contrast, oligoarginine containing C-terminal tryptophan was shown to follow a nonendocytic pathway, independent of energy requirements and temperature [57]. Another type of internalization process has been studied in the bacterium *Clostridium septicum*, whose alpha toxin contains functional domains responsible for oligomerization and cellular pore formation. Using specific domains that bind cell surface receptors, alpha toxin monomers oligomerize to form pores in human cells and thus impose direct entry [58]. By exposing Aβ to endosomal conditions, we were able to observe internalization of A$\beta40/42^{24}$, which was inhibited at 4°C or with the endocytosis inhibitor MDC (Figure 7). Throughout the course of our confocal experiments, we did not observe any disruption of the cell membrane, which would have been expected if membrane channels or pores were being formed by Aβ. Thus, the structural conformation of Aβ that was observed to internalize into cells seems to follow a cell-mediated import mechanism.

Our results with the various Aβ conformations correlate directly with previous reports that indicate the deposition of Aβ in the lysosome [15, 59, 60] and with the previous study that internalized Aβ can persist undegraded for days [61]. From our findings taken together with previous studies, we present the following model for the interaction of Aβ with neuronal cells (Figure 11). As monomeric Aβ binds the cell surface, this event could lead to a conformational change allowing for the further catalytic aggregation of Aβ. Recently, it has been shown that oligomeric Aβ binds to GM1 ganglioside and alters physical properties of the plasma

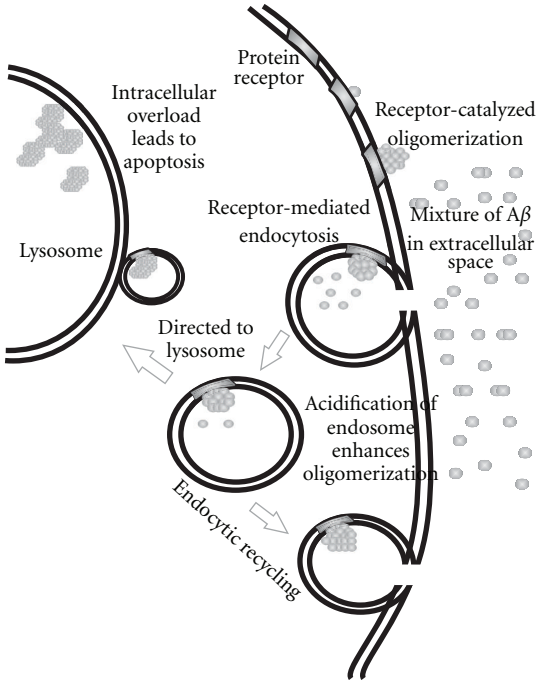

Figure 11: A plausible mechanism of Aβ neurotoxicity.

membrane which stimulates the amyloidogenic processing pathway of APP [62, 63]. Aβ that is bound to the cell surface may become internalized and recycled, allowing for acidification and further aggregation, which in turn may stimulate additional Aβ generation [62]. Once the surface Aβ reach some specific structural form, they may be internalized and directed to the lysosome for potential degradation. However, the reduced pH of the lysosome may instead cause further aggregation and persistence of Aβ, resulting in lysosomal overload and cell death. The recently reported high turnover rate of monomeric Aβ [64, 65] and the formation of large aggregate pools of Aβ may indicate that the human body uses these mechanisms to sequester and remove the toxic Aβ oligomers from neuronal cells. With age, the turnover rate for monomeric Aβ may slow down, which could then result in the initiation of our proposed mechanism and may contribute to the late onset of Alzheimer's disease. It is also possible that endocytosis of Aβ and lysosomal targeting are mechanisms by which the cell clears Aβ aggregates from the cell surface. Also, certain large aggregates of Aβ may just be too large for the cell to internalize, and they may represent the precursor for extracellular Amyloid formation.

5. Conclusion

Our study shows that using a simple method to generate various Aβ conformations, the rates of cellular interaction and targeting can be followed with live cell cultures. Using this model, we found that early endocytic conformations, rather than highly aggregated late forms, serve as the major contributors to rapid cell internalization. The mechanism of internalization likely involves a cell surface receptor-mediated process instead of peptide-mediated direct entry, resulting in accumulation in the lysosome. This method allows for conformation-specific therapeutics and conditions to be screened with live cells, circumventing the need to purify specific Aβ conformations.

Abbreviations

AD:	Alzheimer's disease
Aβ:	Amyloid β
ADDLs:	Aβ-derived diffusible ligands
APP:	Amyloid precursor protein
DAPI:	4′,6-diamidino-2-phenylindole
DMEM/F12:	Dulbecco's modified eagle's medium: nutrient mixture F-12 1 : 1 mixture
D-PBS:	Dulbecco's phosphate-buffered saline
MDC:	Monodansylcadaverine
MWCO:	Molecular weight cut-off
NGF:	Nerve growth factor
PC12:	Rat adrenal pheochromocytoma
TMR:	Tetramethylrhodamine.

Acknowledgments

The authors would like to thank Ms. Silvia Ho for running and analyzing the ultracentrifugation samples. This study was supported by the Neuromuscular Research Partnership—the Canadian Institutes of Health Research, ALS Society (Canada) and Muscular Dystrophy Association (Canada), (AC). D. A. Bateman was supported by a scholarship from NSERC and a SCACE graduate fellowship.

References

[1] G. G. Glenner and C. W. Wong, "Alzheimer's disease: initial report of the purification and characterization of a novel cerebrovascular amyloid protein," *Biochemical and Biophysical Research Communications*, vol. 120, no. 3, pp. 885–890, 1984.

[2] E. H. Koo and S. L. Squazzo, "Evidence that production and release of amyloid β-protein involves the endocytic pathway," *Journal of Biological Chemistry*, vol. 269, no. 26, pp. 17386–17389, 1994.

[3] D. J. Selkoe, "Soluble oligomers of the amyloid β-protein impair synaptic plasticity and behavior," *Behavioural Brain Research*, vol. 192, no. 1, pp. 106–113, 2008.

[4] B. L. Daugherty and S. A. Green, "Endosomal sorting of amyloid precursor protein-P-selectin chimeras influences secretase processing," *Traffic*, vol. 2, no. 12, pp. 908–916, 2001.

[5] M. Shoji, T. E. Golde, J. Ghiso et al., "Production of the Alzheimer amyloid β protein by normal proteolytic processing," *Science*, vol. 258, no. 5079, pp. 126–129, 1992.

[6] W. Xia, W. J. Ray, B. L. Ostaszewski et al., "Presenilin complexes with the C-terminal fragments of amyloid precursor protein at the sites of amyloid β-protein generation," *Proceedings of the National Academy of Sciences of the United States of America*, vol. 97, no. 16, pp. 9299–9304, 2000.

[7] E. H. Koo, S. L. Squazzo, D. J. Selkoe, and C. H. Koo, "Trafficking of cell-surface amyloid β-protein precursor I. Secretion, endocytosis and recycling as detected by labeled

monoclonal antibody," *Journal of Cell Science*, vol. 109, no. 5, pp. 991–998, 1996.

[8] G. C. Peraus, C. L. Masters, and K. Beyreuther, "Late compartments of amyloid precursor protein transport in SY5Y cells are involved in β-amyloid secretion," *Journal of Neuroscience*, vol. 17, no. 20, pp. 7714–7724, 1997.

[9] S. Soriano, A. S. C. Chyung, X. Chen, G. B. Stokin, V. M. Y. Lee, and E. H. Koo, "Expression of β-amyloid precursor protein-CD3γ chimeras to demonstrate the selective generation of amyloid/α and amyloid β peptides within secretory and endocytic compartments," *Journal of Biological Chemistry*, vol. 274, no. 45, pp. 32295–32300, 1999.

[10] C. Haass, E. H. Koo, A. Mellon, A. Y. Hung, and D. J. Selkoe, "Targeting of cell-surface β-amyloid precursor protein to lysosomes: alternative processing into amyloid-bearing fragments," *Nature*, vol. 357, no. 6378, pp. 500–503, 1992.

[11] M. J. Clague, "Molecular aspects of the endocytic pathway," *Biochemical Journal*, vol. 336, no. 2, pp. 271–282, 1998.

[12] D. J. Yamashiro, B. Tycko, S. R. Fluss, and F. R. Maxfield, "Segregation of transferrin to a mildly acidic (pH 6.5) para-Golgi compartment in the recycling pathway," *Cell*, vol. 37, no. 3, pp. 789–800, 1984.

[13] P. M. Gorman, C. M. Yip, P. E. Fraser, and A. Chakrabartty, "Alternate aggregation pathways of the Alzheimer β-amyloid peptide: aβ association kinetics at endosomal pH," *Journal of Molecular Biology*, vol. 325, no. 4, pp. 743–757, 2003.

[14] M. D. Kirkitadze, M. M. Condron, and D. B. Teplow, "Identification and characterization of key kinetic intermediates in amyloid β-protein fibrillogenesis," *Journal of Molecular Biology*, vol. 312, no. 5, pp. 1103–1119, 2001.

[15] A. J. Yang, D. Chandswangbhuvana, L. Margol, and C. G. Glabe, "Loss of endosomal/lysosomal membrane impermeability is an early event in amyloid Aβ1-42 pathogenesis," *Journal of Neuroscience Research*, vol. 52, no. 6, pp. 691–698, 1998.

[16] T. H. J. Huang, D. S. Yang, N. P. Plaskos et al., "Structural studies of soluble oligomers of the Alzheimer β-amyloid peptide," *Journal of Molecular Biology*, vol. 297, no. 1, pp. 73–87, 2000.

[17] M. P. Lambert, A. K. Barlow, B. A. Chromy et al., "Diffusible, nonfibrillar ligands derived from Aβ are potent central nervous system neurotoxins," *Proceedings of the National Academy of Sciences of the United States of America*, vol. 95, no. 11, pp. 6448–6453, 1998.

[18] M. B. Podlisny, D. M. Walsh, P. Amarante et al., "Oligomerization of endogenous and synthetic amyloid β-protein at nanomolar levels in cell culture and stabilization of monomer by Congo red," *Biochemistry*, vol. 37, no. 11, pp. 3602–3611, 1998.

[19] W. B. Stine, S. W. Snyder, U. S. Ladror et al., "The nanometer-scale structure of amyloid-β visualized by atomic force microscopy," *Journal of Protein Chemistry*, vol. 15, no. 2, pp. 193–203, 1996.

[20] D. M. Walsh, D. M. Hartley, Y. Kusumoto et al., "Amyloid β-protein fibrillogenesis. Structure and biological activity of protofibrillar intermediates," *Journal of Biological Chemistry*, vol. 274, no. 36, pp. 25945–25952, 1999.

[21] A. K. Paravastu, I. Qahwash, R. D. Leapman, S. C. Meredith, and R. Tycko, "Seeded growth of β-amyloid fibrils from Alzheimer's brain-derived fibrils produces a distinct fibril structure," *Proceedings of the National Academy of Sciences of the United States of America*, vol. 106, no. 18, pp. 7443–7448, 2009.

[22] D. A. Bateman and A. Chakrabartty, "Two distinct conformations of Aβ aggregates on the surface of living PC12 cells," *Biophysical Journal*, vol. 96, no. 10, pp. 4260–4267, 2009.

[23] Y. Fezoui, D. M. Hartley, J. D. Harper et al., "An improved method of preparing the amyloid β-protein for fibrillogenesis and neurotoxicity experiments," *Amyloid*, vol. 7, no. 3, pp. 166–178, 2000.

[24] D. B. Teplow, "Preparation of amyloid β-protein for structural and functional studies," *Methods in Enzymology*, vol. 413, pp. 20–33, 2006.

[25] S. V. Costes, D. Daelemans, E. H. Cho, Z. Dobbin, G. Pavlakis, and S. Lockett, "Automatic and quantitative measurement of protein-protein colocalization in live cells," *Biophysical Journal*, vol. 86, no. 6, pp. 3993–4003, 2004.

[26] P. Skehan, R. Storeng, D. Scudiero et al., "New colorimetric cytotoxicity assay for anticancer-drug screening," *Journal of the National Cancer Institute*, vol. 82, no. 13, pp. 1107–1112, 1990.

[27] I. Kheterpal, A. Williams, C. Murphy, B. Bledsoe, and R. Wetzel, "Structural features of the Aβ amyloid fibril elucidated by limited proteolysis," *Biochemistry*, vol. 40, no. 39, pp. 11757–11767, 2001.

[28] A. K. Paravastu, R. D. Leapman, W. M. Yau, and R. Tycko, "Molecular structural basis for polymorphism in Alzheimer's β-amyloid fibrils," *Proceedings of the National Academy of Sciences of the United States of America*, vol. 105, no. 47, pp. 18349–18354, 2008.

[29] D. A. Bateman, J. McLaurin, and A. Chakrabartty, "Requirement of aggregation propensity of Alzheimer amyloid peptides for neuronal cell surface binding," *BMC Neuroscience*, vol. 8, article no. 29, 2007.

[30] T. H. J. Huang, P. E. Fraser, and A. Chakrabartty, "Fibrillogenesis of Alzheimer Aβ peptides studied by fluorescence energy transfer," *Journal of Molecular Biology*, vol. 269, no. 2, pp. 214–224, 1997.

[31] P. Sengupta, K. Garai, B. Sahoo, Y. Shi, D. J. E. Callaway, and S. Maiti, "The amyloid β peptide (Aβ) is thermodynamically soluble at physiological concentrations," *Biochemistry*, vol. 42, no. 35, pp. 10506–10513, 2003.

[32] L. O. Tjernberg, A. Pramanik, S. Björling et al., "Amyloid β-peptide polymerization studied using fluorescence correlation spectroscopy," *Chemistry and Biology*, vol. 6, no. 1, pp. 53–62, 1999.

[33] J. D. Harper and P. T. Lansbury, "Models of amyloid seeding in Alzheimer's disease and scrapie: mechanistic truths and physiological consequences of the time-dependent solubility of amyloid proteins," *Annual Review of Biochemistry*, vol. 66, pp. 385–407, 1997.

[34] L. F. Lue, Y. M. Kuo, A. E. Roher et al., "Soluble amyloid β peptide concentration as a predictor of synaptic change in Alzheimer's disease," *American Journal of Pathology*, vol. 155, no. 3, pp. 853–862, 1999.

[35] P. Seubert, C. Vigo-Pelfrey, F. Esch et al., "Isolation and quantification of soluble Alzheimer's β-peptide from biological fluids," *Nature*, vol. 359, no. 6393, pp. 325–327, 1992.

[36] H. LeVine III, "Thioflavine T interaction with synthetic Alzheimer's disease β-amyloid peptides: detection of amyloid aggregation in solution," *Protein Science*, vol. 2, no. 3, pp. 404–410, 1993.

[37] H. LeVine III, "Quantification of β-sheet amyloid fibril structures with thioflavin T," *Methods in Enzymology*, vol. 309, pp. 274–284, 1999.

[38] H. T. Haigler, F. R. Maxfield, M. C. Willingham, and I. Pastan, "Dansylcadaverine inhibits internalization of I-epidermal growth factor in BALB 3T3 cells," *Journal of Biological Chemistry*, vol. 255, no. 4, pp. 1239–1241, 1980.

[39] R. Schlegel, R. B. Dickson, M. C. Willingham, and I. H. Pastan, "Amantadine and dansylcadaverine inhibit vesicular stomatitis virus uptake and receptor-mediated endocytosis of α2-macroglobulin," *Proceedings of the National Academy of Sciences of the United States of America*, vol. 79, no. 7 I, pp. 2291–2295, 1982.

[40] C. Harding, J. Heuser, and P. Stahl, "Receptor-mediated endocytosis of transferrin and recycling of the transferrin receptor in rat reticulocytes," *Journal of Cell Biology*, vol. 97, no. 2, pp. 329–339, 1983.

[41] K. N. Dahlgren, A. M. Manelli, W. Blaine Stine, L. K. Baker, G. A. Krafft, and M. J. Ladu, "Oligomeric and fibrillar species of amyloid-β peptides differentially affect neuronal viability," *Journal of Biological Chemistry*, vol. 277, no. 35, pp. 32046–32053, 2002.

[42] A. Demuro, E. Mina, R. Kayed, S. C. Milton, I. Parker, and C. G. Glabe, "Calcium dysregulation and membrane disruption as a ubiquitous neurotoxic mechanism of soluble amyloid oligomers," *Journal of Biological Chemistry*, vol. 280, no. 17, pp. 17294–17300, 2005.

[43] P. N. Lacor, M. C. Buniel, L. Chang et al., "Synaptic targeting by Alzheimer's-related amyloid β oligomers," *Journal of Neuroscience*, vol. 24, no. 45, pp. 10191–10200, 2004.

[44] H. LeVine III, "Alzheimer's β-peptide oligomer formation at physiologic concentrations," *Analytical Biochemistry*, vol. 335, no. 1, pp. 81–90, 2004.

[45] D. M. Walsh, I. Klyubin, J. V. Fadeeva et al., "Naturally secreted oligomers of amyloid β protein potently inhibit hippocampal long-term potentiation in vivo," *Nature*, vol. 416, no. 6880, pp. 535–539, 2002.

[46] D. B. Freir, R. Fedriani, D. Scully et al., "Aβ oligomers inhibit synapseremodelling necessary for memory consolidation," *Neurobiology of Aging*. In press.

[47] S. Lesné, T. K. Ming, L. Kotilinek et al., "A specific amyloid-β protein assembly in the brain impairs memory," *Nature*, vol. 440, no. 7082, pp. 352–357, 2006.

[48] M. Necula, R. Kayed, S. Milton, and C. G. Glabe, "Small molecule inhibitors of aggregation indicate that amyloid β oligomerization and fibrillization pathways are independent and distinct," *Journal of Biological Chemistry*, vol. 282, no. 14, pp. 10311–10324, 2007.

[49] J. Diaz, P. L. Tornel, and P. Martinez, "Reference intervals for blood ammonia in healthy subjects, determined by microdiffusion," *Clinical Chemistry*, vol. 41, no. 7, p. 1048, 1995.

[50] R. E. Dutton, T. M. Harris, and D. G. Davies, "Distribution of ammonia between blood and cerebrospinal fluid in pulmonary emphysema," *Journal of Applied Physiology*, vol. 36, no. 6, pp. 668–673, 1974.

[51] A. Martinez Hernandez, K. P. Bell, and M. D. Norenberg, "Glutamine synthetase: glial localization in brain," *Science*, vol. 195, no. 4284, pp. 1356–1358, 1977.

[52] M. D. Norenberg, "Histochemical studies in experimental portal systemic encephalopathy. I. Glutamic dehydrogenase," *Archives of Neurology*, vol. 33, no. 4, pp. 265–269, 1976.

[53] A. Deshpande, E. Mina, C. Glabe, and J. Busciglio, "Different conformations of amyloid β induce neurotoxicity by distinct mechanisms in human cortical neurons," *Journal of Neuroscience*, vol. 26, no. 22, pp. 6011–6018, 2006.

[54] J. Hardy and D. J. Selkoe, "The amyloid hypothesis of Alzheimer's disease: progress and problems on the road to therapeutics," *Science*, vol. 297, no. 5580, pp. 353–356, 2002.

[55] R. E. Tanzi, "The synaptic Aβ hypothesis of Alzheimer disease," *Nature Neuroscience*, vol. 8, no. 8, pp. 977–979, 2005.

[56] J. P. Richard, K. Melikov, E. Vives et al., "Cell-penetrating peptides: a reevaluation of the mechanism of cellular uptake," *Journal of Biological Chemistry*, vol. 278, no. 1, pp. 585–590, 2003.

[57] P. E. G. Thorén, D. Persson, P. Isakson, M. Goksör, A. Önfelt, and B. Nordén, "Uptake of analogs of penetratin, Tat(48-60) and oligoarginine in live cells," *Biochemical and Biophysical Research Communications*, vol. 307, no. 1, pp. 100–107, 2003.

[58] J. A. Melton-Witt, L. M. Bentsen, and R. K. Tweten, "Identification of functional domains of Clostridium septicum alpha toxin," *Biochemistry*, vol. 45, no. 48, pp. 14347–14354, 2006.

[59] K. Ditaranto, T. L. Tekirian, and A. J. Yang, "Lysosomal membrane damage in soluble Aβ-mediated cell death in Alzheimer's disease," *Neurobiology of Disease*, vol. 8, no. 1, pp. 19–31, 2001.

[60] R. A. Fuentealba, Q. Liu, J. Zhang et al., "Low-density lipoprotein receptor-related protein 1 (LRP1) mediates neuronal Aβ42 uptake and lysosomal trafficking," *PLoS ONE*, vol. 5, no. 7, article no. e11884, 2010.

[61] D. M. Paresce, H. Chung, and F. R. Maxfield, "Slow degradation of aggregates of the Alzheimer's disease amyloid β-protein by microglial cells," *Journal of Biological Chemistry*, vol. 272, no. 46, pp. 29390–29397, 1997.

[62] I. Peters, U. Igbavboa, T. Schütt et al., "The interaction of beta-amyloid protein with cellular membranes stimulates its own production," *Biochimica et Biophysica Acta - Biomembranes*, vol. 1788, no. 5, pp. 964–972, 2009.

[63] G. P. Eckert, W. G. Wood, and W. E. Müller, "Lipid membranes and β-amyloid: a harmful connection," *Current Protein and Peptide Science*, vol. 11, no. 5, pp. 319–325, 2010.

[64] R. J. Bateman, L. Y. Munsell, J. C. Morris, R. Swarm, K. E. Yarasheski, and D. M. Holtzman, "Human amyloid-β synthesis and clearance rates as measured in cerebrospinal fluid in vivo," *Nature Medicine*, vol. 12, no. 7, pp. 856–861, 2006.

[65] J. R. Cirrito, P. C. May, M. A. O'Dell et al., "In vivo assessment of brain interstitial fluid with microdialysis reveals plaque-associated changes in amyloid-β metabolism and half-life," *Journal of Neuroscience*, vol. 23, no. 26, pp. 8844–8853, 2003.